Does shear flow stabilize an immersed thread?

Does shear flow stabilize an immersed thread?

A.Y. Gunawan[a], J. Molenaar[b], A.A.F. van de Ven[b]

[a]Departemen Matematika, Institut Teknologi Bandung, Indonesia

[b]Department of Mathematics and Computer Science, Eindhoven University of Technology, The Netherlands

Abstract

The stability of one liquid thread immersed in a fluid in a shear field is considered by linear stability analysis. A constant shear stress is imposed far away from the thread. The shear flow tends to deform and elongate the thread. The stability of the thread is characterized by the growth rate of a random perturbation. The equation for the growth rate leads to an eigenvalue problem with the wave number, the ratio of viscosities and the capillary number as parameters. Using *Hurwitz's criterion*, we determine the range of the ratio of viscosities for which the shear stabilizes the thread. A critical capillary number above which the thread is always stable is found. Special attention is paid to the special case of thread and fluid having equal viscosity. Then, the critical capillary number can be calculated analytically.

1 Introduction

In the blending process, relatively big drops of one material are immersed into the shear flow of a second material. The process depends on the magnitude of the capillary number Ca, which is defined as the ratio between the local shear stress Π and the interfacial stress σ/a,

$$\mathrm{Ca} = \frac{a\Pi}{\sigma}, \tag{1}$$

where σ is the surface tension and a is a characteristic radius of the drops in the dispersed phase. Due to dominant shear stresses, long threads are formed. At some moment a thread may become so thin, and thus its radius so small, that the interfacial stress becomes important. Initiated by perturbations, wavy perturbations may develop along the thread. Due to a competition between surface tension and shear flow, these waves may grow in amplitude or attenuate. In an unstable state, the thread will eventually break up into an array of small spherical droplets, whereas in a stable one, the thread will remain undeformed.

The study of the break-up of liquid threads has a distinguished history, starting with the work of Savart [1] in the early nineteenth century. Some years later, Plateau [2] discovered that the source of the break-up is surface tension. The dynamical description of the problem, in terms of linear stability theory, was first given by Rayleigh [3, 4]. He developed the important concept of the *mode of maximum instability*. Rayleigh showed that, from a random perturbation, a number of unstable waves may form on the jet surface; the wave that causes the jet to break up is the one with maximum growth rate. The specific growth rate is referred to as *the* growth rate of the system. In the case of an incompressible, cylindrical column of viscous liquid, assuming

the viscosity to be dominating over the inertia and neglecting the effect of the surrounding fluid, Rayleigh found that the break-up is fastest when the wave length of the perturbation is very large in comparison with the radius of the initial cylinder. Following Rayleigh's approach, Tomotika [5] generalized the analysis to include viscosity for both the fluid column and the surrounding fluid. Tomotika found that if the ratio of viscosities of the two fluids is neither zero nor infinity, the maximum instability always occurs at a definite wave length. A generalization of Tomotika's stability analysis for several limiting cases such as low viscosity liquid jet in a gas, gas jet in a low viscosity liquid, etc., was discussed by Meister and Scheele [6]. Kinoshita et al. [7] derived the equation, which enables much easier prediction of the most unstable wave number and perturbation growth rate than Tomotika's equation. Tomotika [8] also considered the growth of perturbations for the case in which the fluids were not at rest, *i.e.* when the thread is immersed in an extensional flow. For this case, Mikami et al. [9] improved Tomotika's theory theoretically and experimentally. A theoretical study of the break-up of a liquid thread in hyperbolic extensional flow and simple shear flow was analyzed by Khakhar and Ottino [10]. They found that, under similar conditions, the drops produced in simple shear flow are larger than those produced in hyperbolic extensional flow. A wide-ranging review of a large number of theoretical and experimental investigations of the break-up process of one thread is given by Eggers [11].

The stability of a liquid thread in general flow such as hyperbolic extensional flow and simple shear flow was theoretically studied to some extent. For instance, Frischknecht [12] considered the stability of a thread in a phase-separating binary fluid under influence of shear flow. Frischknecht explored the competition between the shear flow and the coarsening process. Using the coupled Cahn-Hilliard and Stokes equations, Frischknecht derived analytically the eigenvalues for long-wavelength perturbations, and showed that the shear flow suppresses and sometimes completely stabilizes both the hydrodynamic Rayleigh instability and the thermodynamic instability of the thread. The results were consistent with a 'string phase' behaviour in phase-separating fluids in shear as observed by Hasimoto et al. [13]. Recent experiments on shear between plates reported by Migler [14] showed that when the size of the droplets becomes comparable to the sample dimension (e.g. gap width between shearing plates), a droplet-string transition is discovered in concentrated polymer blends. Migler proposed that the string state is stabilized by a suppression of the instability due to both finite size effects (for the wider string) and the shear flow (for the narrower one). In a recent paper, assuming that strings can be simply viewed as droplets with a large aspect ratio, Pathak and Migler [15] found that confinement not only promoted deformation, but also allowed larger stable droplets (strings) to exist under flow. They then concluded that strings may be stabilized by a combination of shear flow and confinement.

In Gunawan et al. [16, 17], we studied the stability of liquid threads immersed in a fluid in an unconfined region and driven by surface tension. It was shown that the instability of the threads is determined by the wave number k of the perturbations, the viscosity ratio μ of the two fluids and the distance b between the threads. In this paper, we investigate the hydrodynamics stability of a Newtonian thread immersed in another fluid, if a constant shear stress Π_0 is present far away from the thread. The fluids are assumed to be incompressible and so viscous that the creeping flow approximation is applicable. The thread is perturbed by a random perturbation. The perturbation and the quantities such as pressure and velocity fields are expressed as a complex

Fourier series in the azimuthal coordinate and they are taken periodic in the axial coordinate with real wave number k. At the interfaces, we correct the boundary conditions derived by Frischknecht [12]. Here, we show that the velocity in the axial coordinate has a discontinuity due to the presence of the shear flow. The equation for the growth rate of some sinusoidal perturbation leads to an eigenvalue problem with the wave number of the perturbation, the ratio of viscosities between two fluids and the capillary number as parameters. Using *Hurwitz's criterion*, we find a range for the ratio of viscosities for which the shear stabilizes the thread. Although we make some corrections with respect to the boundary conditions as derived by Frischknecht [12] and follow a completely different approach, we find qualitatively comparable results. Due to these corrections, somewhat modified results for the range of the ratio of the viscosities in which no instability will occur are obtained.

The paper is organized as follows. In Section 2, we derive the mathematical model and the boundary conditions. Here, we consider a Couette-like flow problem as the unperturbed solution. For the perturbed solution, we solve the Stokes equation together with the equation of continuity via separation of variables. In this, the dependence on the azimuthal coordinate is written in the form of complex Fourier expansions, and that on the axial coordinate is written as a periodic function with real wave number k. In Section 3, the stability is studied for two cases: in the absence and in the presence of shear. The former is included as a check for our method since the data are available in literature. Special attention is paid to the stability of fluids having matching viscosity. For this case, we derive an analytical formula for the critical applied stress above which the thread is always stable. Conclusions are written in Section 4.

2 Mathematical formulation and solution methodology

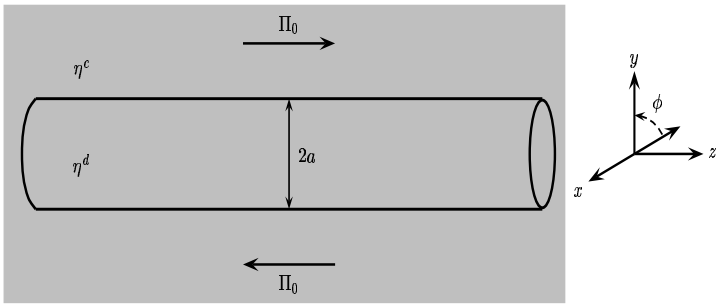

Figure 1: *Thread immersed in a fluid in shear flow.*

Let us consider a single thread of radius a with viscosity η^d, immersed in an infinite region filled with fluid with viscosity η^c. We define

$$\mu = \frac{\eta^d}{\eta^c} \ , \tag{2}$$

as the ratio of viscosities of the fluids. The indices c and d stand for the continuous phase (the surrounding fluid) and the disperse phase (the thread), respectively. We introduce cylindrical coordinates with the z-axis along the thread axis. As sketched in Figure 1, an external flow is

imposed along the z-direction by applying a constant shear stress Π_0 far away from the thread. The shear takes place in the (y, z)-plane.

As unperturbed state, we take the thread to be a perfect cylinder. Its stability is tested by applying a random perturbation. The perturbed thread surface is represented by

$$R(t,\phi,z) = a[1+\epsilon f(t,\phi,z)] \quad \text{with} \quad f(t,\phi,z) = \Re\Big[\sum_{m=-\infty}^{\infty} \varepsilon_m(t) e^{i(m\phi+kz)}\Big]. \tag{3}$$

Here, $i = \sqrt{-1}$ is the imaginary unit and $\Re$ the real part symbol. We express the perturbation as a complex Fourier series in ϕ and take it periodic in z with wave number k. Since the solution is periodic in the z-direction, k must be real. The ε_m are the time-dependent perturbation amplitudes and ϵ is a small, but further irrelevant, parameter ($0 < \epsilon \ll 1$). Note that ε_m is assumed to be a complex quantity. In the sequel, we shall not write the '$\Re$'-symbol explicitly, as is common practice in the analysis of complex-valued fields.

The fluids are assumed to be Newtonian, incompressible, and so viscous that inertial effects are negligible. So, the system is governed by the creeping flow approximation:

$$\text{div } \mathbf{u} = 0, \tag{4a}$$

$$\text{div } \boldsymbol{\tau} = \mathbf{0}, \tag{4b}$$

where $\mathbf{u}$ is the velocity field and $\boldsymbol{\tau}$ the total stress tensor. Since we are interested in the stability of the system, we write the solution in the form

$$\begin{aligned} &\mathbf{u} = \mathbf{V} + \epsilon\mathbf{v}, \quad \boldsymbol{\tau} = \boldsymbol{\Pi} + \epsilon\boldsymbol{\pi}, \\ &\boldsymbol{\Pi} = -P\boldsymbol{\delta} + \boldsymbol{\Gamma}, \quad \boldsymbol{\pi} = -p\boldsymbol{\delta} + \boldsymbol{\tau}, \end{aligned} \tag{5}$$

where $\mathbf{V} = (U, V, W)$ is the unperturbed velocity, with U, V, and W the velocity components in radial, azimuthal, and axial directions, respectively, $\boldsymbol{\Pi}$ the unperturbed total stress tensor, P the unperturbed pressure, $\boldsymbol{\delta}$ the unit tensor and $\boldsymbol{\Gamma}$ the unperturbed extra stress tensor. Variables $\mathbf{v} = (u, v, w)$, $\boldsymbol{\pi}$ and $\boldsymbol{\tau}$ are the perturbations of $\mathbf{V}, \boldsymbol{\Pi}$ and $\boldsymbol{\Gamma}$, respectively. For Newtonian fluids, we have (T indicates the transpose)

$$\boldsymbol{\tau} = \widehat{\eta}\,[\text{grad } \mathbf{v} + (\text{grad } \mathbf{v})^T]. \tag{6}$$

Here, $\widehat{\eta}$ is the viscosity, where $\widehat{\eta} = \eta^d$ for the thread and $\widehat{\eta} = \eta^c$ for the surrounding fluid. Substituting (5) and (6) into (4), we obtain equations for the perturbed and unperturbed systems. The unperturbed state depends on the problem considered. In the present work, the unperturbed state is the Couette-like flow problem. For the perturbed state, we find from (4), (5) and (6)

$$0 = \text{div } \mathbf{v}\ , \tag{7a}$$

$$\text{grad } p = \widehat{\eta}\ \text{div } (\text{grad } \mathbf{v})^T\ . \tag{7b}$$

Note that grad $\mathbf{v} \equiv (\nabla\mathbf{v})^T$. The formulation (7) is a coordinate-free notation.

2.1 Boundary conditions

As for the boundary conditions at the interface, we require continuity of velocity, the dynamical conditions for the stresses, and a kinematic condition expressing that the thread surface is a material surface.

The detailed evaluation of the boundary conditions is as follows. The continuity of the velocity is written as

$$[\![\mathbf{u}]\!] = \mathbf{0}. \tag{8}$$

Here, $[\![g]\!] = g^d - g^c$ denotes the jump of an arbitrary function g across the interface. Evaluating $\mathbf{u} = \mathbf{u}(r, \phi, z, t)$ at the interface $r = a + \epsilon a f$, we find (suppressing the dependence on ϕ, z and t for convenience)

$$\begin{aligned} \mathbf{u}(a + \epsilon a f) &= (\mathbf{V} + \epsilon \mathbf{v})(a + \epsilon a f) \\ &= (\mathbf{V} + \epsilon \mathbf{v})(a) + \epsilon a f \frac{\partial}{\partial r}\Big[\mathbf{V} + \epsilon \mathbf{v}\Big](a) + O(\epsilon^2) \\ &= \mathbf{V}(a) + \epsilon\Big[\mathbf{v}(a) + a f \frac{\partial \mathbf{V}}{\partial r}(a)\Big] + O(\epsilon^2). \end{aligned} \tag{9}$$

Substitution of (9) into (8) yields for the unperturbed ($\mathrm{O}(\epsilon^0)$) and the perturbed ($\mathrm{O}(\epsilon^1)$) terms,

$$\epsilon^0 : \quad [\![\mathbf{V}(a)]\!] = 0, \tag{10a}$$

$$\epsilon^1 : \quad \Big[\!\Big[\mathbf{v}(a) + a f \frac{\partial \mathbf{V}}{\partial r}(a)\Big]\!\Big] = 0. \tag{10b}$$

Next, we formulate conditions for the stresses. The outward unit normal $\mathbf{n} = \mathrm{n}_r \mathbf{e}_r + \mathrm{n}_\phi \mathbf{e}_\phi + \mathrm{n}_z \mathbf{e}_z$ at the interface is given by

$$\begin{aligned} \mathbf{n} &= \frac{1}{\sqrt{1 + \left(\epsilon \frac{a}{R}\frac{\partial f}{\partial \phi}\right)^2 + \left(\epsilon a \frac{\partial f}{\partial z}\right)^2}} \left[\mathbf{e}_r - \epsilon \frac{a}{R}\frac{\partial f}{\partial \phi}\mathbf{e}_\phi - \epsilon a \frac{\partial f}{\partial z}\mathbf{e}_z\right] \\ &= \mathbf{e}_r - \epsilon \frac{\partial f}{\partial \phi}\mathbf{e}_\phi - \epsilon a \frac{\partial f}{\partial z}\mathbf{e}_z + \boldsymbol{O}(\epsilon^2). \end{aligned} \tag{11}$$

Here, $\mathbf{e}_r$, $\mathbf{e}_\phi$ and $\mathbf{e}_z$ are the unit base vectors in radial, azimuthal and axial direction, respectively. Two unit tangent vectors on the perturbed interface, orthogonal to $\mathbf{n}$ and to each other (up to $O(\epsilon^2)$), are

$$\mathbf{t}_1 = \epsilon \frac{\partial f}{\partial \phi}\mathbf{e}_r + \mathbf{e}_\phi + \boldsymbol{O}(\epsilon^2), \tag{12a}$$

$$\mathbf{t}_2 = \epsilon a \frac{\partial f}{\partial z}\mathbf{e}_r + \mathbf{e}_z + \boldsymbol{O}(\epsilon^2). \tag{12b}$$

The stress vector $\mathbf{g}$ at the interface is given by

$$\mathbf{g} = \boldsymbol{\tau}\mathbf{n} = (\boldsymbol{\Pi} + \epsilon \boldsymbol{\pi})\mathbf{n}. \tag{13}$$

Substituting (11) into (13), we find the $r-$, $\phi-$ and $z-$ components of $\mathbf{g}$ at the interface:

$$\mathrm{g}_r = \Pi_{rr}(a) + \epsilon\left[\pi_{rr}(a) + af\frac{\partial \Pi_{rr}}{\partial r}(a) - \Pi_{r\phi}(a)\frac{\partial f}{\partial \phi} - a\Pi_{rz}(a)\frac{\partial f}{\partial z}\right] + O(\epsilon^2), \tag{14a}$$

$$\mathrm{g}_\phi = \Pi_{r\phi}(a) + \epsilon\left[\pi_{r\phi}(a) + af\frac{\partial \Pi_{r\phi}}{\partial r}(a) - \Pi_{\phi\phi}(a)\frac{\partial f}{\partial \phi} - a\Pi_{z\phi}(a)\frac{\partial f}{\partial z}\right] + O(\epsilon^2), \tag{14b}$$

$$\mathrm{g}_z = \Pi_{rz}(a) + \epsilon\left[\pi_{rz}(a) + af\frac{\partial \Pi_{rz}}{\partial r}(a) - \Pi_{z\phi}(a)\frac{\partial f}{\partial \phi} - a\Pi_{zz}(a)\frac{\partial f}{\partial z}\right] + O(\epsilon^2). \tag{14c}$$

The dynamical boundary conditions require that

$$[\![\mathbf{g}\cdot\mathbf{t}]\!] = 0, \tag{15a}$$

$$[\![\mathbf{g}\cdot\mathbf{n}]\!] = -\sigma\left(\frac{1}{R_1} + \frac{1}{R_2}\right). \tag{15b}$$

Here, σ is the surface tension (in Newton/meter), and R_1 and R_2 are the principle radii of curvature, defined as

$$\begin{aligned}
\frac{1}{R_1} &= -\frac{\dfrac{\partial^2 R}{\partial z^2}}{\left[1+\left(\dfrac{\partial R}{\partial z}\right)^2\right]^{3/2}} = -\epsilon a\frac{\partial^2 f}{\partial z^2} + O(\epsilon^2),\\
\frac{1}{R_2} &= \frac{R^2 + 2\left(\dfrac{\partial R}{\partial \phi}\right)^2 - R\dfrac{\partial^2 R}{\partial^2 \phi}}{\left[R^2+\left(\dfrac{\partial R}{\partial \phi}\right)^2\right]^{3/2}} = \frac{1}{a}\left[1-\epsilon\left(f+\frac{\partial^2 f}{\partial^2\phi}\right)\right] + O(\epsilon^2).
\end{aligned} \tag{16}$$

So, (15a) represents continuity of the tangential component of the stress vector $\mathbf{g}$, and (15b) discontinuity of its normal component. Note that the jump in the normal stress is balanced by the surface tension. The minus sign at the right-hand side of (15b) follows the convention in Chandrasekhar [18]. Substituting (12a) and (12b) into (15a), we obtain

$$\epsilon^0: \quad [\![\Pi_{r\phi}]\!] = 0, \quad [\![\Pi_{rz}]\!] = 0, \tag{17a}$$

$$\epsilon^1: \quad \left[\!\!\left[\pi_{r\phi} + af\frac{\partial \Pi_{r\phi}}{\partial r} + \left[\Pi_{rr} - \Pi_{\phi\phi}\right]\frac{\partial f}{\partial \phi} - a\Pi_{z\phi}\frac{\partial f}{\partial z}\right]\!\!\right] = 0, \tag{17b}$$

$$\epsilon^1: \quad \left[\!\!\left[\pi_{rz} + af\frac{\partial \Pi_{rz}}{\partial r} - \Pi_{z\phi}\frac{\partial f}{\partial \phi} + a\left[\Pi_{rr} - \Pi_{zz}\right]\frac{\partial f}{\partial z}\right]\!\!\right] = 0. \tag{17c}$$

From (15b), we find

$$\epsilon^0: \quad [\![\Pi_{rr}]\!] = -\frac{\sigma}{a}, \tag{18a}$$

$$\epsilon^1: \quad \left[\!\!\left[\pi_{rr} + af\frac{\partial \Pi_{rr}}{\partial r} - 2\Pi_{r\phi}\frac{\partial f}{\partial \phi} - 2a\Pi_{rz}\frac{\partial f}{\partial z}\right]\!\!\right] = \frac{\sigma}{a}\left[f + a^2\frac{\partial^2 f}{\partial z^2} + \frac{\partial^2 f}{\partial \phi^2}\right]. \tag{18b}$$

Note that from now on the jump $[\![\cdot]\!]$ is evaluated at $r = a$, since we have developed the perturbed boundary conditions with respect to the unperturbed state. In doing this, we only maintained first-order terms in the perturbations. Hence, we apply linear stability theory. Using (5) and (6), we can rewrite (17) and (18) in terms of the pressure and the velocities, as will be done in the next section.

The kinematic condition requires that at the perturbed interface $R(\phi, z, t)$, being a material surface, the radial velocity is given by the material derivative (DR/Dt) following a thread particle:

$$\mathbf{u}^d \cdot \mathbf{e}_r = \frac{DR}{Dt} = \frac{\partial R}{\partial t} + (\mathbf{u}^d \cdot \mathbf{e}_\phi)\frac{1}{R}\frac{\partial R}{\partial \phi} + (\mathbf{u}^d \cdot \mathbf{e}_z)\frac{\partial R}{\partial z}. \tag{19}$$

2.2 The unperturbed solution

We assume that there is no pressure gradient present in the unperturbed state; we only prescribe a constant shear stress Π_0, far away from the thread (see in Figure 1). This implies that the pressure P is a constant, apart from a possible jump at the thread surface. Thus, for this state we obtain

$$\text{div } \mathbf{V} = 0 \ , \tag{20a}$$

$$\text{div } (\text{grad } \mathbf{V})^T = \mathbf{0}, \tag{20b}$$

supplemented by the condition at infinity (the shear at infinity is in the (y, z)-plane)

$$\mathbf{V} \longrightarrow (0, 0, \frac{\Pi_0}{\eta^c} y)^T = (0, 0, \frac{\Pi_0}{\eta^c} r \sin\phi)^T = \left(0, 0, \Re\left\{-i\frac{\Pi_0}{\eta^c} r e^{i\phi}\right\}\right)^T. \tag{21}$$

We try $\mathbf{V} = (0, 0, W(r, \phi))$ with $W(r, \phi) = -iG(r)e^{i\phi}$ satisfying (20). For later convenience, the factor $-i$ is added. Then, we find that the general solution of (20) is given by

$$W(r, \phi) = -i\left(Ar + \frac{B}{r}\right)e^{i\phi}. \tag{22}$$

The constants A and B are to be determined from the boundary conditions, and take different values in the two phases. The boundary conditions in $O(\epsilon^0)$ are

$$[\![W]\!] = 0, \tag{23a}$$

$$[\![\Pi_{rz}]\!] = [\![\Gamma_{rz}]\!] = 0 \tag{23b}$$

$$[\![\Pi_{rr}]\!] = [\![-P]\!] = -\frac{\sigma}{a}. \tag{23c}$$

Note that the other boundary conditions at the interface are obviously satisfied. We also have two more conditions, *i.e.* the solution must remain bounded at the origin, and for $r \to \infty$ we prescribe, according to (21), $W \to -i\Pi_0 r e^{i\phi}/\eta^c$. Evaluating the boundary conditions, we find

$$W = \begin{cases} -i\dfrac{2\Pi_0}{\eta^c(1+\mu)} r e^{i\phi} \quad ; \quad 0 \le r \le a, \\ -i\dfrac{\Pi_0}{\eta^c}\left[r + \dfrac{1-\mu}{1+\mu}\dfrac{a^2}{r}\right]e^{i\phi} \quad ; \quad r \ge a, \end{cases} \tag{24}$$

and

$$P = \begin{cases} P_0 + \dfrac{\sigma}{a}, & 0 \le r \le a, \\ \\ P_0, & r \ge a, \end{cases} \tag{25}$$

with P_0 being a further irrelevant constant. For convenience, the equations will be brought into dimensionless form. The distance, velocity, and stress components are made dimensionless with respect to a, σ/η^c, and σ/a, respectively. For example, we have

$$\begin{aligned} &r = ar^*, \quad z = az^*, \quad R = aR^*, \quad \mathbf{u} = \frac{\sigma}{\eta^c}\mathbf{u}^*, \quad \boldsymbol{\tau} = \frac{\sigma}{a}\boldsymbol{\tau}^*, \\ &p = \frac{\sigma}{a}p^*, \quad t = \frac{a\eta^c}{\sigma}t^*, \quad \text{and} \quad k = \frac{k^*}{a}. \end{aligned} \tag{26}$$

In the sequel we omit the stars, since confusion is not possible. For the velocity W, substitution of (26) into (24) yields

$$W = \begin{cases} -i\dfrac{2\mathrm{Ca}}{1+\mu} r e^{i\phi} \quad ; \quad 0 \le r \le 1, \\ -i\mathrm{Ca}\left[r + \dfrac{1-\mu}{1+\mu}\dfrac{1}{r}\right] e^{i\phi} \quad ; \quad r \ge 1. \end{cases} \tag{27}$$

Here, we have introduced the capillary number Ca as

$$\mathrm{Ca} = \frac{\Pi_0 a}{\sigma}. \tag{28}$$

We also calculate the derivative of W with respect to r:

$$\frac{\partial W}{\partial r} = \begin{cases} -i\dfrac{2\mathrm{Ca}}{1+\mu} e^{i\phi} \quad ; \quad 0 \le r \le 1, \\ -i\mathrm{Ca}\left[1 - \dfrac{1-\mu}{1+\mu}\dfrac{1}{r^2}\right] e^{i\phi} \quad ; \quad r \ge 1. \end{cases} \tag{29}$$

Note that (29) has a discontinuity at $r = 1$, except for $\mu = 1$. From (27) we calculate the unperturbed stress components as

$$\begin{aligned} &\Pi_{rr} = \Pi_{\phi\phi} = \Pi_{zz} = \begin{cases} \dfrac{-P_0 a}{\sigma} - 1 \quad ; \quad 0 \le r \le 1, \\ \dfrac{-P_0 a}{\sigma} \quad ; \quad r \ge 1, \end{cases} \\ &\Gamma_{r\phi} = 0, \\ &\Gamma_{rz} = \begin{cases} -i\dfrac{2\mu\mathrm{Ca}}{1+\mu} e^{i\phi} \quad ; \quad 0 \le r \le 1, \\ -i\mathrm{Ca}\left[1 - \dfrac{1-\mu}{1+\mu}\dfrac{1}{r^2}\right] e^{i\phi} \quad ; \quad r \ge 1, \end{cases} \\ &\Gamma_{z\phi} = \begin{cases} \dfrac{2\mu\mathrm{Ca}}{1+\mu} e^{i\phi} \quad ; \quad 0 \le r \le 1, \\ \mathrm{Ca}\left[1 + \dfrac{1-\mu}{1+\mu}\dfrac{1}{r^2}\right] e^{i\phi} \quad ; \quad r \ge 1, \end{cases} \end{aligned} \tag{30}$$

We note that at the interface $r = 1$ the shear stress Γ_{rz} is continuous (as it should be), but this does not hold for $\Gamma_{z\phi}$, except for $\mu = 1$.

2.3 The perturbed solution

From (7) with $\mathbf{v} = u\mathbf{e}_r + v\mathbf{e}_\phi + w\mathbf{e}_z$, we find that the perturbations u, v, w and p satisfy a set of four equations (in cylindrical coordinates):

$$0 = \frac{1}{r}\frac{\partial\,[ru]}{\partial r} + \frac{1}{r}\frac{\partial v}{\partial \phi} + \frac{\partial w}{\partial z}, \tag{31a}$$

$$\frac{\partial p}{\partial r} = \widehat{\eta}\left[\frac{1}{r}\frac{\partial}{\partial r}\left[r\frac{\partial u}{\partial r}\right] + \frac{1}{r^2}\frac{\partial^2 u}{\partial \phi^2} + \frac{\partial^2 u}{\partial z^2} - \frac{2}{r^2}\frac{\partial v}{\partial \phi} - \frac{u}{r^2}\right], \tag{31b}$$

$$\frac{1}{r}\frac{\partial p}{\partial \phi} = \widehat{\eta}\left[\frac{1}{r}\frac{\partial}{\partial r}\left[r\frac{\partial v}{\partial r}\right] + \frac{1}{r^2}\frac{\partial^2 v}{\partial \phi^2} + \frac{\partial^2 v}{\partial z^2} + \frac{2}{r^2}\frac{\partial u}{\partial \phi} - \frac{v}{r^2}\right], \tag{31c}$$

$$\frac{\partial p}{\partial z} = \widehat{\eta}\left[\frac{1}{r}\frac{\partial}{\partial r}\left[r\frac{\partial w}{\partial r}\right] + \frac{1}{r^2}\frac{\partial^2 w}{\partial \phi^2} + \frac{\partial^2 w}{\partial z^2}\right]. \tag{31d}$$

We propose as general expressions for the solution, the expansions

$$p = \sum_{m=-\infty}^{\infty} p_m(r,t)e^{i(m\phi+kz)}, \tag{32a}$$

$$u = \sum_{m=-\infty}^{\infty} u_m(r,t)e^{i(m\phi+kz)}, \tag{32b}$$

$$v = \sum_{m=-\infty}^{\infty} -iv_m(r,t)e^{i(m\phi+kz)}, \tag{32c}$$

$$w = \sum_{m=-\infty}^{\infty} -iw_m(r,t)e^{i(m\phi+kz)}. \tag{32d}$$

Here, we have added an extra factor $-i$ to v_m and w_m for later convenience. In these formulae we should read the right-hand sides as preceded by the 'real part of'. Substitution of (32) into

(31) yields the equations for the coefficients:

$$0 = \frac{1}{r}\frac{\partial\left[ru_m\right]}{\partial r} + \frac{m}{r}v_m + kw_m, \tag{33a}$$

$$\frac{\partial p_m}{\partial r} = \widehat{\eta}\left[\frac{1}{r}\frac{\partial}{\partial r}\left[r\frac{\partial u_m}{\partial r}\right] - \frac{m^2+1+(kr)^2}{r^2}u_m - \frac{2m}{r^2}v_m\right], \tag{33b}$$

$$-\frac{m}{r}p_m = \widehat{\eta}\left[\frac{1}{r}\frac{\partial}{\partial r}\left[r\frac{\partial v_m}{\partial r}\right] - \frac{m^2+1+(kr)^2}{r^2}v_m - \frac{2m}{r^2}u_m\right], \tag{33c}$$

$$-kp_m = \widehat{\eta}\left[\frac{1}{r}\frac{\partial}{\partial r}\left[r\frac{\partial w_m}{\partial r}\right] - \frac{m^2+(kr)^2}{r^2}w_m\right]. \tag{33d}$$

To solve (33), we use the same analysis as in Gunawan et al. [19]. The solution for the dispersed phases reads

$$p_m^d(r,t) = 2\mu A_m I_m(kr)\ , \tag{34a}$$

$$u_0^d(r,t) = A_0 r I_0(kr) - \left[B_0 + \frac{2}{k}A_0\right] I_1(kr)\ , \tag{34b}$$

$$u_m^d(r,t) = A_m r I_m(kr) - \left[B_m + \frac{1}{k}(m+2)A_m\right] I_{m+1}(kr) + \frac{C_m}{r}I_m(kr)\ , \tag{34c}$$

$$v_0^d(r,t) = C_0 I_1(kr)\ , \tag{34d}$$

$$v_m^d(r,t) = -\left[B_m + \frac{1}{k}(m+2)A_m + \frac{k}{m}C_m\right] I_{m+1}(kr) - \frac{1}{r}C_m I_m(kr)\ , \tag{34e}$$

$$w_m^d(r,t) = -A_m r I_{m+1}(kr) + B_m I_m(kr)\ . \tag{34f}$$

and for the continuous phase

$$p_m^c(r,t) = 2D_m K_m(kr)\ , \tag{35a}$$

$$u_0^c(r,t) = D_0 r K_0(kr) + \left[E_0 + \frac{2}{k}D_0\right] K_1(kr)\ , \tag{35b}$$

$$u_m^c(r,t) = D_m r K_m(kr) + \left[E_m + \frac{1}{k}(m+2)D_m\right] K_{m+1}(kr) + \frac{F_m}{r}K_m(kr)\ , \tag{35c}$$

$$v_0^c(r,t) = F_0 K_1(kr)\ , \tag{35d}$$

$$v_m^c(r,t) = \left[E_m + \frac{1}{k}(m+2)D_m + \frac{k}{m}F_m\right] K_{m+1}(kr) - \frac{1}{r}F_m K_m(kr)\ , \tag{35e}$$

$$w_m^c(r,t) = D_m r K_{m+1}(kr) + E_m K_m(kr)\ . \tag{35f}$$

However, in a comparison of Gunawan et al. [19] with the present solution, one essential difference appears; as the present problem is not rotationally symmetric, the assumption $v_0 = 0$ does not hold anymore.

Next, we evaluate the boundary conditions at the interface for the perturbed fields. From Section 2.1, we obtain for the $O(\epsilon^1)$-contributions,

$$[\![u]\!] = 0, \tag{36a}$$

$$[\![v]\!] = 0, \tag{36b}$$

$$[\![w]\!] = -\left[\!\!\left[f\frac{\partial W}{\partial r} \right]\!\!\right], \tag{36c}$$

$$[\![\tau_{r\phi}]\!] = \left[\!\!\left[\widehat{\eta}\left(\frac{\partial u}{\partial \phi} + \frac{\partial v}{\partial r} - v \right) \right]\!\!\right] = \left[\!\!\left[\Gamma_{z\phi}\frac{\partial f}{\partial z} \right]\!\!\right], \tag{36d}$$

$$[\![\tau_{rz}]\!] = \left[\!\!\left[\widehat{\eta}\left(\frac{\partial u}{\partial z} + \frac{\partial w}{\partial r} \right) \right]\!\!\right] = \left[\!\!\left[\Gamma_{z\phi}\frac{\partial f}{\partial \phi} \right]\!\!\right] - \left[\!\!\left[\frac{\partial \Gamma_{rz}}{\partial r} f \right]\!\!\right], \tag{36e}$$

$$[\![\tau_{rr}]\!] = \left[\!\!\left[-p + 2\widehat{\eta}\frac{\partial u}{\partial r} \right]\!\!\right] = \left[f + \frac{\partial^2 f}{\partial^2 z} + \frac{\partial^2 f}{\partial^2 \phi} \right]. \tag{36f}$$

Note that the jump in (36c) and the second term in the right-hand side of (36e) were incorrectly not included by Frischknecht [12]. This correction gives noticeable results for the range of ratios of viscosities above which the thread is stable, as we will discuss in the next section. In terms of the components of the expansions (32), (36) becomes

$$[\![u_m]\!] = 0, \tag{37a}$$

$$[\![v_m]\!] = 0, \tag{37b}$$

$$[\![w_m]\!] = \mathrm{Ca}\frac{\mu - 1}{\mu + 1}\left(\varepsilon_{m-1} - \varepsilon_{m+1} \right), \tag{37c}$$

$$\left[\!\!\left[\widehat{\eta}\left(m u_m - \frac{\partial v_m}{\partial r} + v_m \right) \right]\!\!\right] = k\mathrm{Ca}\frac{\mu - 1}{\mu + 1}\left(\varepsilon_{m-1} + \varepsilon_{m+1} \right), \tag{37d}$$

$$\left[\!\!\left[\widehat{\eta}\left(k u_m - \frac{\partial w_m}{\partial r} \right) \right]\!\!\right] = m\mathrm{Ca}\frac{\mu - 1}{\mu + 1}\left(\varepsilon_{m-1} + \varepsilon_{m+1} \right), \tag{37e}$$

$$\left[\!\!\left[-p_m + 2\widehat{\eta}\frac{\partial u_m}{\partial r} \right]\!\!\right] = (1 - k^2 - m^2)\varepsilon_m. \tag{37f}$$

Next, we consider the evolution in time of the perturbation amplitude $\varepsilon_m(t)$. At the perturbed interface $R(\phi, z, t)$, the radial velocity is the material derivative (DR/Dt) following a thread particle (see (19)). Since at the interface $\mathbf{V}^d = (0, 0, W^d)$, we obtain from (19) (with

$\mathbf{u}^d = W^d \mathbf{e}_z + \epsilon\ (u^d \mathbf{e}_r + v^d \mathbf{e}_\phi + w^d \mathbf{e}_z))$

$$\epsilon\ u^d = \frac{\partial R}{\partial t} + \epsilon\ v^d \frac{\partial R}{\partial \phi} + (W^d + \epsilon\ w^d) \frac{\partial R}{\partial z}. \tag{38}$$

Using (3) for R and (32b) for u^d in (38), we obtain for the term linear in ϵ,

$$\sum_{m=-\infty}^{\infty} u_m^d e^{i(m\phi+kz)} = \sum_{m=-\infty}^{\infty} \frac{d\varepsilon_m}{dt} e^{i(m\phi+kz)} + ikW^d \sum_{m=-\infty}^{\infty} \varepsilon_m e^{i(m\phi+kz)}\ . \tag{39}$$

Now, W^d is given by the first equation of (27), however, with the restriction that we have to take the real part of this. This yields, for $r = 1$,

$$W^d = -i\frac{\mathrm{Ca}}{\mu+1}\left(e^{i\phi} - e^{-i\phi}\right)\ . \tag{40}$$

Substituting this into (39), rearranging terms, and equating equal powers of $e^{i\phi}$, we arrive at

$$\frac{d}{dt}\varepsilon_m(t) = u_m^d - \frac{k\mathrm{Ca}}{\mu+1}\left(\varepsilon_{m-1} - \varepsilon_{m+1}\right), \quad \text{for } m \in (-\infty, \infty). \tag{41}$$

In practice, the series (3) is cut off at $m = \pm M$, say. So, we have $(2M+1)$ terms from $m = -M$ to $m = M$. Note that in order to satisfy the boundary conditions (37c)-(37e), the solution must be cut off one order higher, *i.e.* at $m = \pm(M+1)$.

3 Stability analysis

Equations (41) contain the information about the time evolution of the initial perturbation. In this section, we shall work this out for several cases. First, we take the cut off value M equal to $M = 0$. This corresponds to the case that the cross-sections of the thread remain perfectly circular for all z. This inevitably implies that this case can not incorporate the effect of the shear flow. We only report this case in order to compare the present approach with results in the literature. The emphasis is on the $M = 1$ case, for which the shear flow is really relevant.

3.1 The $M = 0$ case

In this case, $\varepsilon_0 \neq 0$ and $\varepsilon_m = 0$ for $m = \pm 1, \pm 2, \cdots$. From (41), the amplitude $\varepsilon_0(t)$ evolves according to

$$\frac{d}{dt}\varepsilon_0(t) = u_0^d. \tag{42}$$

Evaluating (37), we can formally write the result as

$$\mathbf{Mz} \equiv \begin{pmatrix} \mathbf{M}_{-1} & \mathbf{0} & \mathbf{0} \\ \mathbf{0} & \mathbf{M}_0 & \mathbf{0} \\ \mathbf{0} & \mathbf{0} & \mathbf{M}_1 \end{pmatrix} \begin{pmatrix} \mathbf{z}_{-1} \\ \mathbf{z}_0 \\ \mathbf{z}_1 \end{pmatrix} = \begin{pmatrix} \mathbf{e}_{-1} \\ \mathbf{e}_0 \\ \mathbf{e}_1 \end{pmatrix}. \tag{43}$$

Here, $\mathbf{z}_m = (A_m, B_m, C_m, D_m, E_m, F_m)^T$, $m = -1, 0, 1$, and

$$\mathbf{e}_{-1} = \left(0, 0, -\mathrm{Ca}\frac{\mu-1}{\mu+1}\varepsilon_0, k\mathrm{Ca}\frac{\mu-1}{\mu+1}\varepsilon_0, -\mathrm{Ca}\frac{\mu-1}{\mu+1}\varepsilon_0, 0\right)^T, \tag{44a}$$

$$\mathbf{e}_0 = \left(0, 0, 0, 0, 0, (1-k^2)\varepsilon_0\right)^T, \tag{44b}$$

$$\mathbf{e}_1 = \left(0, 0, \mathrm{Ca}\frac{\mu-1}{\mu+1}\varepsilon_0, k\mathrm{Ca}\frac{\mu-1}{\mu+1}\varepsilon_0, \mathrm{Ca}\frac{\mu-1}{\mu+1}\varepsilon_0, 0\right)^T. \tag{44c}$$

For simplicity, we shall write $\mathbf{M}$ as a diagonal block matrix; $\mathbf{M} = \mathrm{diag}(\mathbf{M}_{-1}, \mathbf{M}_0, \mathbf{M}_1)$. Thus, we may solve the equation via

$$\mathbf{M}_m \mathbf{z}_m = \mathbf{e}_m, \ m = -1, 0, 1. \tag{45}$$

Expressions for $\mathbf{M}_m$ are given in the Appendix. Since u_0^d only depends on A_0 and B_0 (see (34b)) we may solve these coefficients from (43) by only considering

$$\mathbf{M}_0 \mathbf{z}_0 = \mathbf{e}_0. \tag{46}$$

Solving (46), we find that u_0^d is proportional to ε_0. Substituting this value into (42), we obtain

$$\frac{d}{dt}\varepsilon_0(t) = q_0(k, \mu)\varepsilon_0(t), \tag{47}$$

where

$$q_0(k, \mu) = \frac{(k^2-1)}{|\mathbf{M}_0|}\left[\left(I_0(k) - \frac{2}{k}I_1(k)\right)|\mathbf{M}_0^{6,1}| + I_1(k)|\mathbf{M}_0^{6,2}|\right]. \tag{48}$$

Here, $|\cdot|$ denotes the determinant and $\mathbf{M}_0^{i,j}$ is the 5×5 sub-matrix of $\mathbf{M}_0$, which is obtained

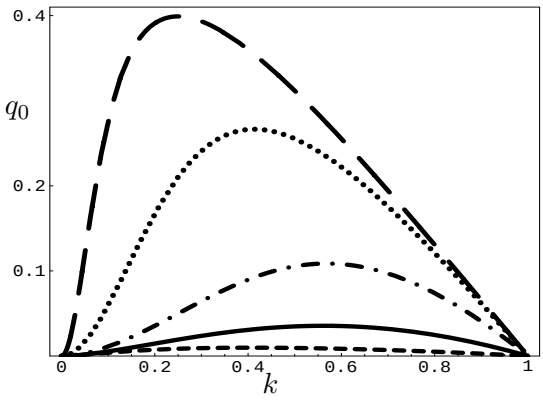

Figure 2: *Curves of q_0 as function of k for different μ values; $\mu = 10$ (dashed curve), $\mu = 1$ (solid curve), $\mu = 0.1$ (dash-dot curve), $\mu = 0.01$ (dotted curve), and $\mu = 0.001$ (long dashed curve).*

by omitting the i-th row and the j-th column of $\mathbf{M}_0$. The factor q_0 is shown in Figure 2 as a function of k. Note that for $k > 1$, always $q_0 < 0$. Here, $q_0(\mu, k)$ corresponds to the growth rate of the amplitude of the axisymmetric mode. From this figure, we see that $q_0 > 0$ for all μ and this indicates instability. If μ increases, the values of q_0 decrease. Thus, the more viscous the thread, the longer it takes to disintegrate. If the thread is very viscous, it will remain undeformed for a long time before finally breaking up into droplets of very small size. Similar results were reported earlier by Tomotika [5], Mikami et al. [9] and Frischknecht [12]. Remark that the values of q_0 differ from the results of Frischknecht [12] by a factor of 2/3, due to a different scaling of the surface tension σ.

3.2 The $M = 1$ case

Here, we take $\varepsilon_m \neq 0$, for $m = -1, 0, 1$. Equations (41) give

$$\frac{d}{dt}\varepsilon_{-1}(t) = u^d_{-1} + \frac{k\mathrm{Ca}}{\mu+1}\varepsilon_0(t), \tag{49a}$$

$$\frac{d}{dt}\varepsilon_0(t) = u^d_0 - \frac{k\mathrm{Ca}}{\mu+1}\Big(\varepsilon_{-1}(t) - \varepsilon_1(t)\Big), \tag{49b}$$

$$\frac{d}{dt}\varepsilon_1(t) = u^d_1 - \frac{k\mathrm{Ca}}{\mu+1}\varepsilon_0(t). \tag{49c}$$

Evaluation of the boundary conditions leads to (45) with $m = -2, \cdots, 2$. Expressions for u^d_{-1}, u^d_0 and u^d_1 are given in (34b) and (34c), while the coefficients in these expressions follow from

$$\mathbf{M}_m\mathbf{z}_m = \mathbf{e}_m, \ m = -1, 0, 1, \tag{50}$$

with $\mathbf{z}_m = (A_m, B_m, C_m, D_m, E_m, F_m)^T$ and

$$\mathbf{e}_{-1} = \left(0, 0, -\mathrm{Ca}\frac{\mu-1}{\mu+1}\varepsilon_0, k\mathrm{Ca}\frac{\mu-1}{\mu+1}\varepsilon_0, -\mathrm{Ca}\frac{\mu-1}{\mu+1}\varepsilon_0, -k^2\varepsilon_{-1}\right)^T, \tag{51a}$$

$$\mathbf{e}_0 = \left(0, 0, \mathrm{Ca}(\mu-1)(\varepsilon_{-1} - \varepsilon_1)/(\mu+1), k\mathrm{Ca}(\mu-1)(\varepsilon_{-1} + \varepsilon_1)/(\mu+1), 0, (1-k^2)\varepsilon_0\right)^T, \tag{51b}$$

$$\mathbf{e}_1 = \left(0, 0, \mathrm{Ca}\frac{\mu-1}{\mu+1}\varepsilon_0, k\mathrm{Ca}\frac{\mu-1}{\mu+1}\varepsilon_0, \mathrm{Ca}\frac{\mu-1}{\mu+1}\varepsilon_0, -k^2\varepsilon_1\right)^T. \tag{51c}$$

In (50) we wrote down the equation only for $m = -1, 0$ and 1, since the evolution equation (49) only contains $\varepsilon_{-1}, \varepsilon_0$ and ε_1. The analogon of (47) reads here

$$\frac{d\mathbf{y}}{dt} = \mathbf{Q}(k, \mu, \mathrm{Ca})\mathbf{y}, \qquad \mathbf{Q} \equiv \begin{pmatrix} q_{11} & q_{12} & 0 \\ q_{21} & q_{22} & q_{23} \\ 0 & q_{32} & q_{33} \end{pmatrix}, \tag{52}$$

where $\mathbf{y} \equiv (\varepsilon_{-1}(t), \varepsilon_0(t), \varepsilon_1(t))^T$, while the q_{ij}'s are given in the Appendix. Note that the q_{ij}'s are real. They generally depend on k, μ and Ca, but the diagonal elements of $\mathbf{Q}$ are independent of Ca. The presence of the shear flow leads to a coupling of modes via the non-diagonal elements. The behaviour of the solution of (52) depends on the sign of the real parts of the eigenvalues of the matrix $\mathbf{Q}$. If all eigenvalues have negative real parts, the unperturbed solution is stable. If at least one of the eigenvalues has a positive real part, the unperturbed solution is unstable. Let q be an eigenvalue of $\mathbf{Q}$, satisfying the equation

$$q^3 + a_1 q^2 + a_2 q + a_3 = 0, \tag{53}$$

where the coefficients a_j are real and depend on k, μ and Ca. Expressions for a_j in terms of q_{ij} are written out in the Appendix. To find the necessary and sufficient conditions for the coefficients a_j for which all roots of (53) to have negative real parts, we will use *Hurwitz's criterion*. This criterion says that all roots of the third-order algebraic equation (53) have negative real parts, if and only if (see Merkin [20])

$$a_1 > 0, \quad a_2 > 0, \quad a_3 > 0, \quad a_4 = a_1 a_2 - a_3 > 0. \tag{54}$$

If one of the inequalities in (54) is reversed, then at least one of the roots of equation (53) will have a positive real part, and this is an indication of instability of the system. For fixed values μ and Ca, we should realize that the inequalities (54) must hold for *all* wave numbers k.

As a check, we first calculate the growth rate of the perturbations in the absence of shear flow. Next, we investigate the effect of shear flow on the stability of the thread.

3.2.1 No shear flow (Ca = 0)

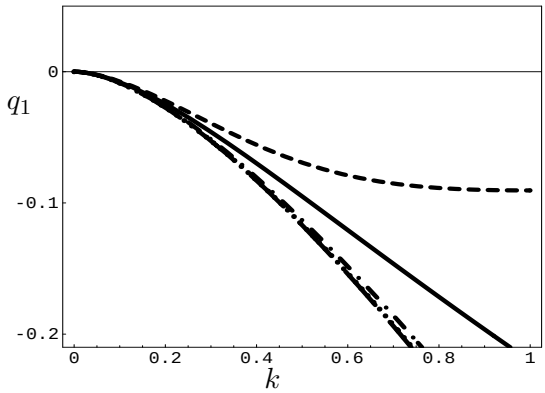

Figure 3: *Same information as in Figure 2, but now for* q_1.

For this case, $\mathbf{Q}$ is diagonal and the eigenvalues of $\mathbf{Q}$ are thus given by $q_0(\mu, k) = q_{22}$ and $q_1(\mu, k) = q_{11} = q_{33}$. Here, $q_0(\mu, k)$ corresponds to the growth rate of the amplitude of the axisymmetric mode (see Figure 2), and $q_1(\mu, k)$ corresponds to the growth rate of the amplitude of the first non-axisymmetric mode. The curves of $q_1(\mu, k)$ as a function of k are shown in Figure 3, for the same μ-values as in Figure 2. Figure 3 shows that q_1 is negative for all k. Thus, this mode always decays. If we extend the mode to $m = 2$ ($\mathbf{Q}$ in (52) now becomes a 4 by 4 diagonal

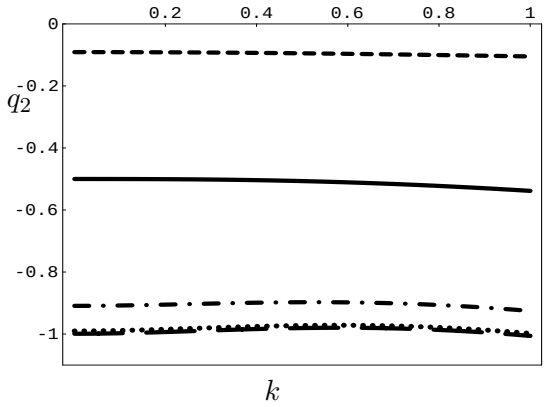

Figure 4: *Same information as in Figure 2, but now for q_2.*

matrix), we can also calculate the growth rate q_2 of the second non-axisymmetric mode. The results are shown in Figure 4. Again, we see that the $m = 2$ mode is negative. So, we conclude that in the no-shear flow case the thread is unstable since the axisymmetric $m = 0$ mode is unstable.

We now proceed by considering the peculiar case $k = 0$, in which the perturbed thread remains uniform in z-direction and in which there is no displacement in this direction. Due to incompressibility (here requiring conservation of area for the cross-section), the cross-section can only deform in a non-axisymmetric mode with $m \geq 2$ (the mode $m = 1$ only gives a rigid-body translation). For this special case, we see from Figures 2 and 3 that indeed the growth rates vanish for $m = 0$ and $m = 1$. However, this is not the case for $m = 2$, as we can see from Figure 4. For $m \geq 2$, we can calculate the growth rate analytically, providing a check on the numerical results. For $m \geq 2$, we obtain the following solutions for $r < 1$,

$$u_m^d(r,t) = A_m r^{m-1} + \frac{m}{2(m+1)} B_m r^{m+1}, \tag{55a}$$

$$v_m^d(r,t) = -A_m r^{m-1} - \frac{m+2}{2(m+1)} B_m r^{m+1}, \tag{55b}$$

$$w_m^d(r,t) = 0, \tag{55c}$$

$$p_m^d(r,t) = 2\mu B_m r^m, \tag{55d}$$

and for $r > 1$,

$$u_m^c(r,t) = C_m r^{-(m+1)} + \frac{m}{2(m-1)} D_m r^{-(m-1)} \ , \tag{56a}$$

$$v_m^c(r,t) = C_m r^{-(m+1)} + \frac{m-2}{2(m-1)} D_m r^{-(m-1)} \ , \tag{56b}$$

$$w_m^c(r,t) = 0, \tag{56c}$$

$$p_m^c(r,t) = 2D_m r^{-m} \ . \tag{56d}$$

Evaluating the boundary conditions, we obtain the linear system

$$\mathbf{M}_{m;k=0}\mathbf{z}_m = \mathbf{e}_m, \tag{57}$$

with $\mathbf{z}_m = (A_m, B_m, C_m, D_m)^T$ and $\mathbf{e}_m = (0, 0, 0, (1-m^2)\varepsilon_m)^T$. The expression for $\mathbf{M}_{m;k=0}$ is given in the Appendix. Using (55a) and (57), we again obtain (47), but now with

$$q_m(\mu; k=0) = -\frac{m}{2(1+\mu)}, \quad m \geq 2. \tag{58}$$

Since the growth rate is negative, the thread will not break up with a non-circular cross section that is uniform along z-direction.

3.2.2 Shear flow effects (Ca $\neq 0$)

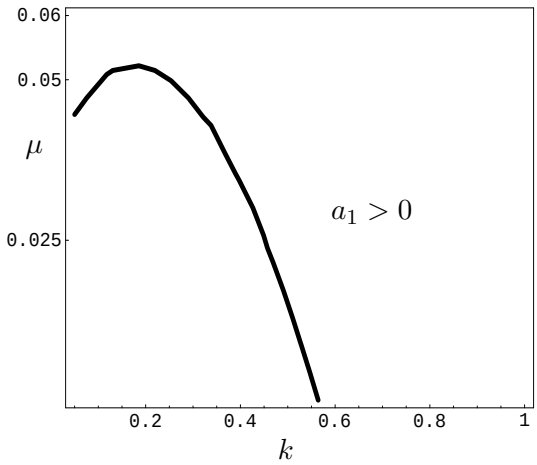

Figure 5: *Curve defined by the relation $a_1(k, \mu) = 0$ in the (k, μ)-plane.*

We shall use (54) to determine a critical value Ca_{cr} of Ca, above which the thread is stable. Since a_1 in (53) is only determined by the diagonal elements of the matrix $\mathbf{Q}$, which do not depend on Ca (see the Appendix), also a_1 does not depend on Ca: $a_1 = a_1(k, \mu)$. The curve $a_1(k, \mu) = 0$ is shown in Figure 5. Below this curve, $a_1(k, \mu) < 0$, and above it $a_1(k, \mu) > 0$. Here and in the sequel, it should be understood that the curve is the border between the regions of positive and the negative values for the coefficients (here a_1). Figure 5 shows that the curve has a maximum value at $\mu_a \approx 0.05$. If $\mu < \mu_a$, then there exist values for k for which $a_1(k, \mu) < 0$. This indicates that the perturbed thread is unstable. If $\mu > \mu_a$, then the perturbed thread may be stabilized by the imposed shear flow. However, then we should also check the other coefficients, a_2, a_3 and a_4; the results are shown in Figure 6. These Figures show the curves $a_i(k, \mu, \mathrm{Ca}) = 0$, for $i = 2, 3, 4$, for fixed value of μ, yielding Ca as a function of k for two different values of μ ($\mu = 0.1$ and $\mu = 0.15$). Part (a) shows that the curves $a_2 = 0$ and $a_3 = 0$ cross each other at $k = k_s$, say. Thus, $a_2(k_s, 0.1, \mathrm{Ca}) = 0 = a_3(k_s, 0.1, \mathrm{Ca})$. Substituting these values into (54), we see that also $a_4(k_s, 0.1, \mathrm{Ca}) = 0$, and this curve is drawn as a vertical line in Figure 6. In this case, no critical value for Ca above which the thread is stable exists, since there are for

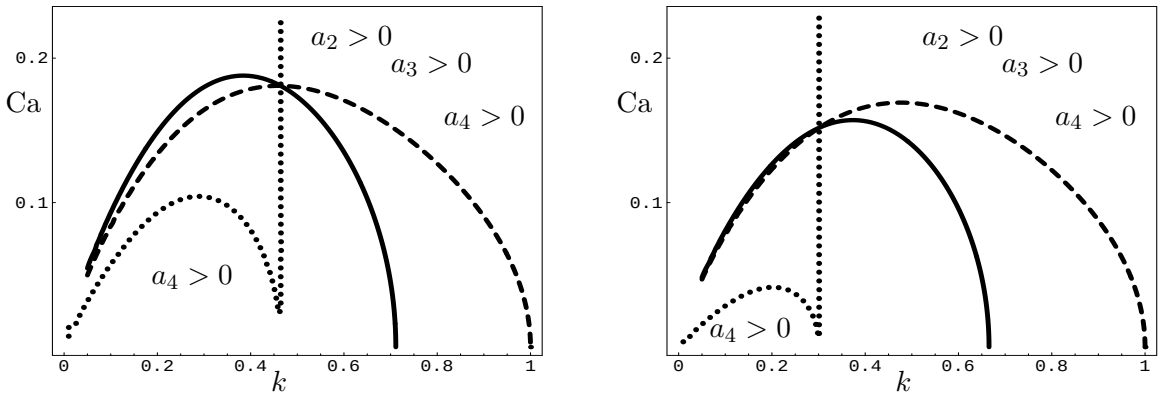

(a) $\mu = 0.1$. (b) $\mu = 0.15$.

Figure 6: *Curves defined by the relations* $a_2(k, \mu, \mathrm{Ca}) = 0$ *(solid line),* $a_3(k, \mu, \mathrm{Ca}) = 0$ *(dashed line), and* $a_4(k, \mu, \mathrm{Ca}) = 0$ *(dotted line) in the* (k, Ca) *plane for two values of* μ*.*

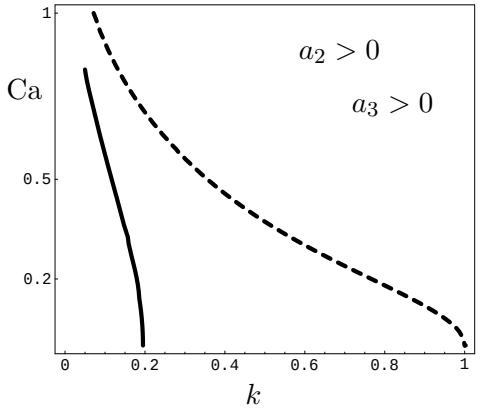

Figure 7: *Same information as in Figure 6, but now for* $\mu = 3.0$*.*

every value of Ca always values of k for which one or more of the coefficients a_2, a_3 or a_4 become negative. If μ increases, k_s decreases; see Figure 6(b). Thus, the window $0 \leq k \leq k$ in which $a_4 < 0$ becomes narrower. However, increasing μ too far we again obtain instability as shown in Figure 7. From this figure, we see that at the left a small window of k is always present for which the coefficients a_2 and a_3 have negative values. From more detailed calculations we find that no instability will occur if $0.18 \leq \mu \leq 2.9$. This range is much larger than the one found by Frischknecht [12] ($0.8 \leq \mu \leq 1.0$), due to the correction in the derivation of the boundary conditions we found, as mentioned in Section 2.3. Hence, for $0.18 \leq \mu \leq 2.9$ we can determine a critical Capillary number Ca_{cr}, as we shall show next. Note that for this range the values of a_4 are always positive for all k's. As an illustration, we investigate the system for which the fluids have no viscosity difference, so $\mu = 1$. Figure 8 shows the curves $a_2 = 0$ and $a_3 = 0$ in the (k, Ca)-plane for $\mu = 1$. The solid and the dashed curves depict the values of $a_2 = 0$ and $a_3 = 0$, respectively. We find a critical value of Ca, $\mathrm{Ca}_{cr} \approx 0.16$, above which the thread will be stable for all wave numbers k. Figure 9 shows the critical capillary number Ca_{cr} as a function

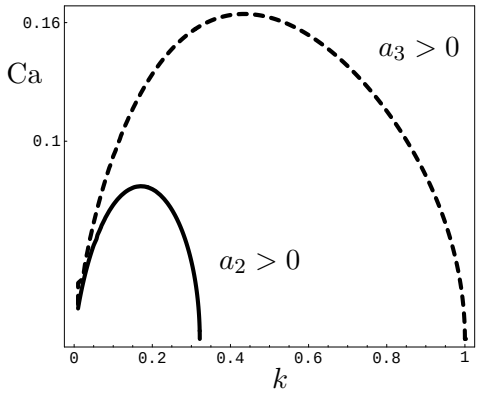

Figure 8: *Same information as in Figure 6, but now for* $\mu = 1$.

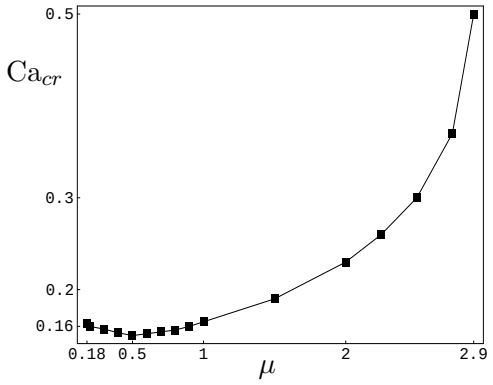

Figure 9: *Critical capillary number* Ca_{cr} *as a function of the ratio of viscosities* μ.

of the ratio of viscosities μ. We see that Ca_{cr} has a minimum near $\mu = 0.5$. So, if the viscosity of the thread is about half the viscosity of the surrounding medium, high stresses are needed to stabilize the thread.

In general, we must include the higher-order modes into the calculations in order to ensure convergence of the truncated system. The more higher modes, the bigger the size of the matrix $\mathbf{Q}$ in (52) will be. Then, calculations become cumbersome. However, we may estimate the number of modes that gives reliable results as follows. In the absence of shear flow, the matrix $\mathbf{Q}$ is diagonal. The only mode that gives instability is the axisymmetric mode; see Section 3.1. From (41), we see that, since the boundary conditions (37) are proportional to Ca the off-diagonal elements of $\mathbf{Q}$ are all proportional to Ca. The presence of shear flow leads to a coupling of modes via this off-diagonal. Thus, we only need to include modes whose damping rates are less than or of the order of the applied shear rate. Formula (58) specifies the behaviour of the damping rates of high m modes.

3.3 Critical capillary number for $\mu = 1$

If the fluids have equal viscosities, *i.e.* $\mu = 1$, the only non-vanishing interfacial condition is the condition for the normal stress (37f). The jump in the normal stress across the interface can

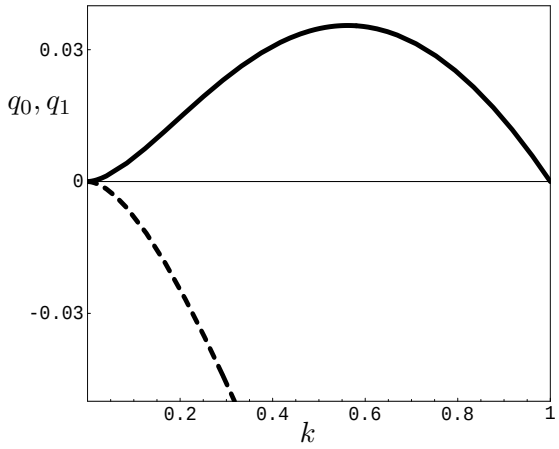

Figure 10: *Curves of q_0 (solid line) and q_1 (dashed line) as function of k, for $\mu = 1$.*

now be incorporated by introducing it as a discrete hoop force S,

$$S = \sum_{m=-\infty}^{\infty} (1 - k^2 - m^2)\varepsilon_m(t) e^{i(m\phi + kz)}, \tag{59}$$

acting only on the interfacial surface $r = 1$. This way, the governing equations can be declared to hold in the whole space (for every $r \in [0, \infty)$), where S is introduced as a body force characterized by a Dirac delta function, $\delta(r-1)$. The perturbed state is then governed by, for $r \geq 0$,

$$0 = \text{div } \mathbf{v} \ , \tag{60a}$$

$$\text{grad } p = \widehat{\eta} \ \text{div } (\text{grad } \mathbf{v})^T + S \ \delta(r-1) \ \mathbf{e}_r \ . \tag{60b}$$

The detailed derivation of the solution of (60) can be found in Gunawan et al. [21]; here we only present the result. The solution for the radial velocity reads

$$\begin{aligned} u_m \ = \ & \frac{(1 - k^2 - m^2)\varepsilon_m}{4} \left[\int_0^{\infty} \frac{s^3 + 2k^2 s}{(s^2 + k^2)^2} \Big(J_{m+1}(s) J_{m+1}(sr) + J_{m-1}(s) J_{m-1}(sr) \Big) ds \right. \\ & \left. + \ \int_0^{\infty} \frac{s^3}{(s^2 + k^2)^2} \Big(J_{m-1}(s) J_{m+1}(sr) + J_{m+1}(s) J_{m-1}(sr) \Big) ds \right] . \end{aligned} \tag{61}$$

For $r > 1$ the integrals can be analytically evaluated (see [22, Formula 13.53(6)]) and we obtain

$$\begin{aligned} u_m \ = \ & \frac{(1 - k^2 - m^2)}{4} \varepsilon_m \left[\frac{1}{2k} \frac{d}{dk} \left[k^2 \Big(I_{m+1}(k) K_{m+1}(kr) + I_{m-1}(k) K_{m-1}(kr) \Big) \right] \right. \\ & - k \frac{d}{dk} \Big[I_{m+1}(k) K_{m+1}(kr) + I_{m-1}(k) K_{m-1}(kr) \Big] \\ & \left. - \frac{1}{2k} \frac{d}{dk} \left[k^2 \Big(I_{m-1}(k) K_{m+1}(kr) + I_{m+1}(k) K_{m-1}(kr) \Big) \right] \right] . \end{aligned} \tag{62}$$

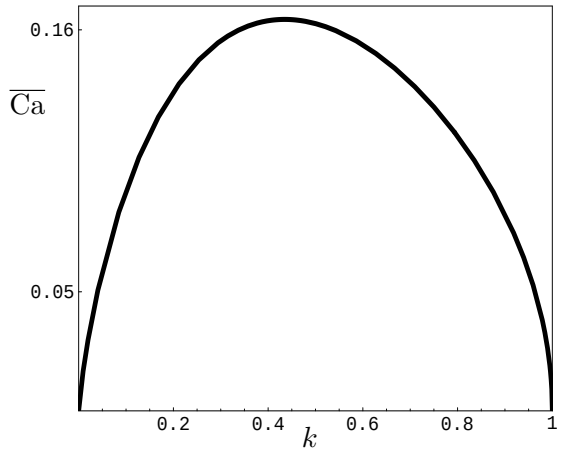

Figure 11: *Curve of* $\overline{\mathrm{Ca}}$ *as a function of* k*, for* $\mu = 1$*. The maximum value of* $\overline{\mathrm{Ca}}$ *indicates the critical capillary number* Ca_{cr}*.*

Let us consider the evolution equation (52). For $\mu = 1$, the matrix $\mathbf{Q}$ becomes

$$\mathbf{Q} \equiv \begin{pmatrix} q_1 & \dfrac{k\mathrm{Ca}}{2} & 0 \\ -\dfrac{k\mathrm{Ca}}{2} & q_0 & \dfrac{k\mathrm{Ca}}{2} \\ 0 & -\dfrac{k\mathrm{Ca}}{2} & q_1 \end{pmatrix}, \tag{63}$$

where $q_m = u_m(r=1)/\varepsilon_m$, with u_m given by (62). In (63), we have used that $q_{-1} = q_1$. Figure 10 shows the curves of q_0 and q_1 as functions of k, for $0 \le k \le 1$. Note that the values of q_0 are positive, whereas the values of q_1 are negative.

Let us denote the modulus of q_m by $|q_m|$, $m = 0, 1$. The eigenvalues of (63) satisfy equation (53), with the coefficients given by

$$a_1 = 2|q_1| - |q_0|, \tag{64a}$$

$$a_2 = |q_1|^2 - |q_0 q_1| + \left(\frac{k^2\mathrm{Ca}^2}{2} - |q_0 q_1|\right), \tag{64b}$$

$$a_3 = |q_1|\left(\frac{k^2\mathrm{Ca}^2}{2} - |q_0 q_1|\right). \tag{64c}$$

From Figure 10, we see that $|q_1| > |q_0|$. So, the coefficients a_m $(m = 1, 2, 3)$ will be positive if and only if the term inside the brackets is positive, that is if

$$\frac{k^2\mathrm{Ca}^2}{2} - |q_0 q_1| > 0. \tag{65}$$

Using that $a_4 = a_1 a_2 - a_3$, we find from (64) that

$$a_4 = \Big(2|q_1| - |q_0|\Big)\Big(|q_1|^2 - |q_0 q_1|\Big) + \Big(|q_1| - |q_0|\Big)\left(\frac{k^2\mathrm{Ca}^2}{2} - |q_0 q_1|\right) > 0, \tag{66}$$

provided that (65) holds. Thus, we may define the critical capillary number Ca_{cr} as,

$$\mathrm{Ca}_{cr} = \max\left\{ \frac{\sqrt{2|q_0 q_1|}}{k} \;\middle|\; 0 < k < 1 \right\}. \tag{67}$$

Let us define $\overline{\mathrm{Ca}}(k) = \sqrt{2|q_0 q_1|}/k$. Figure 11 shows the curve of $\overline{\mathrm{Ca}}$ as a function of k. The maximum value of $\overline{\mathrm{Ca}}$ gives the critical capillary number Ca_{cr}. For this special case, we find $\mathrm{Ca}_{cr} \approx 0.164$.

4 Conclusions

In this paper, we have studied the stability of a Newtonian thread immersed in a Newtonian fluid in a shear field. The system is governed by the Stokes equations and the relevant dimensionless numbers are the ratio of the viscosities μ of the thread and the surrounding fluid, the wave number k of the perturbation, and the capillary number Ca. We have solved these equations by means of complex Fourier expansions and shown that the growth rate follows from an eigenvalue problem. The stability was investigated by use of *Hurwitz's* criterion. We found that the shear flow stabilizes the thread only in the window $0.18 \leq \mu \leq 2.9$. The results presented here explain the stability of the "narrower string" observed by Migler [14].

From the view of polymer blending the present results may provide important insights for control of the production process, such as droplet-string transition in immiscible sheared polymer blends. By use of a critical capillary number found here, one may define a critical radius for the string formation.

Acknowledgement

This research is supported by QUE-Project (IBRD Loan No.4193-IND) of Departemen Matematika, Institut Teknologi Bandung, Indonesia.

Appendix

Here, the prime denotes the derivation with respect to k.

$$\mathbf{M}_0 = \begin{pmatrix}
I_0(k) - \frac{2}{k} I_1(k) & -I_1(k) & 0 & -[K_0(k) + \frac{2}{k} K_1(k)] & -K_1(k) & 0 \\
0 & 0 & I_1(k) & 0 & 0 & -K_1(k) \\
-I_1(k) & I_0(k) & 0 & -K_1(k) & -K_0(k) & 0 \\
0 & 0 & \mu(I_1(k) - kI_1'(k)) & 0 & 0 & -K_1(k) + kK_1'(k) \\
\mu k I_1'(k) & -\mu k I_1(k) & 0 & k K_1'(k) & -k K_1(k) & 0 \\
2\mu\left[kI_1(k) - 2I_1'(k)\right] & -2\mu k I_1'(k) & 0 & -2\left[2K_1'(k) - kK_1(k)\right] & -2kK_1'(k) & 0
\end{pmatrix}$$

$$
\mathbf{M}_m = \left(
\begin{array}{cc}
I_m(k) - \dfrac{m+2}{k} I_{m+1}(k) & -I_{m+1}(k) \\
-\dfrac{m+2}{k} I_{m+1}(k) & -I_{m+1}(k) \\
-I_{m+1}(k) & I_m(k) \\
\mu\Big[m I_m(k) - \dfrac{(m+1)(m+2)}{k} I_{m+1}(k) + (m+2) I'_{m+1}(k) \Big] & \mu\Big[k I'_{m+1}(k) - (m+1) I_{m+1}(k) \Big] \\
\mu[k I_m(k) - (m+1) I_{m+1}(k) + k I'_{m+1}(k)] & -\mu k [I_{m+1}(k) + I'_m(k)] \\
2\mu \left[k I'_m(k) - (m+2) I'_{m+1}(k) \right] & -2\mu k I'_{m+1}(k)
\end{array}
\right.
$$

$$
\begin{array}{cc}
I_m(k) & -\Big[K_m(k) + \dfrac{m+2}{k} K_{m+1}(k) \Big] \\
-\dfrac{k}{m} I_{m+1}(k) - I_m(k) & -\dfrac{m+2}{k} K_{m+1}(k) \\
0 & -K_{m+1}(k) \\
\mu\Big[(m-2) I_m(k) - \dfrac{k}{m} I_{m+1}(k) + k I'_m(k) + \dfrac{k^2}{m} I'_{m+1}(k) \Big] & -\Big[m K_m(k) + \dfrac{(m+1)(m+2)}{k} K_{m+1}(k) - (m+2) K'_{m+1}(k) \Big] \\
\mu k I_m(k) & -[k K_m(k) + (m+1) K_{m+1}(k) - k K'_{m+1}(k)] \\
2\mu [k I'_m(k) - I_m(k)] & -2 \left[k K'_m(k) + (m+2) K'_{m+1}(k) \right]
\end{array}
$$

$$
\begin{array}{cc}
-K_{m+1}(k) & -K_m(k) \\
-K_{m+1}(k) & -\Big[\dfrac{k}{m} K_{m+1}(k) - K_m(k) \Big] \\
-K_m(k) & 0 \\
-\Big[-k K'_{m+1}(k) + (m+1) K_{m+1}(k) \Big] & -\Big[(m-2) K_m(k) + \dfrac{k}{m} K_{m+1}(k) + k K'_m(k) - \dfrac{k^2}{m} K'_{m+1}(k) \Big] \\
-k [K_{m+1}(k) - K'_m(k)] & -k K_m(k) \\
-2 k K'_{m+1}(k) & -2 [k K'_m(k) - K_m(k)]
\end{array}
\right)
$$

$$
\begin{aligned}
q_{11} &= \frac{k^2}{|\mathbf{M}_{-1}|}\left[\left(I_1(k)-\frac{1}{k}I_0(k)\right)|\mathbf{M}_{-1}^{6,1}|+I_0(k)|\mathbf{M}_{-1}^{6,2}|+I_1(k)|\mathbf{M}_{-1}^{6,3}|\right],\\
q_{12} &= -\frac{\mathrm{Ca}}{|\mathbf{M}_{-1}|}\frac{\mu-1}{\mu+1}\left[\left(I_1(k)-\frac{1}{k}I_0(k)\right)\left(|\mathbf{M}_{-1}^{3,1}|+|\mathbf{M}_{-1}^{5,1}|\right)\right.\\
&\qquad\left.+I_0(k)\left(|\mathbf{M}_{-1}^{3,2}|+|\mathbf{M}_{-1}^{5,2}|\right)+I_1(k)\left(|\mathbf{M}_{-1}^{3,3}|+|\mathbf{M}_{-1}^{5,3}|\right)\right]\\
&\quad-\frac{k\mathrm{Ca}}{|\mathbf{M}_{-1}|}\frac{\mu-1}{\mu+1}\left[\left(I_1(k)-\frac{1}{k}I_0(k)\right)|\mathbf{M}_{-1}^{4,1}|+I_0(k)|\mathbf{M}_{-1}^{4,2}|+I_1(k)|\mathbf{M}_{-1}^{4,3}|\right]\\
&\quad+\frac{k\mathrm{Ca}}{\mu+1},\\
q_{21} &= \frac{\mathrm{Ca}}{|\mathbf{M}_0|}\frac{\mu-1}{\mu+1}\left[\left(I_0(k)-\frac{2}{k}I_1(k)\right)|\mathbf{M}_0^{3,1}|+I_1(k)|\mathbf{M}_0^{3,2}|\right]\\
&\quad-\frac{k\mathrm{Ca}}{|\mathbf{M}_0|}\frac{\mu-1}{\mu+1}\left[\left(I_0(k)-\frac{2}{k}I_1(k)\right)|\mathbf{M}_0^{4,1}|+I_1(k)|\mathbf{M}_0^{4,2}|\right]-\frac{k\mathrm{Ca}}{\mu+1},\\
q_{22} &= \frac{k^2-1}{|\mathbf{M}_0|}\left[\left(I_0(k)-\frac{2}{k}I_1(k)\right)|\mathbf{M}_0^{6,1}|+I_1(k)|\mathbf{M}_0^{6,2}|\right],\\
q_{23} &= -\frac{\mathrm{Ca}}{|\mathbf{M}_0|}\frac{\mu-1}{\mu+1}\left[\left(I_0(k)-\frac{2}{k}I_1(k)\right)|\mathbf{M}_0^{3,1}|+I_1(k)|\mathbf{M}_0^{3,2}|\right]\\
&\quad-\frac{k\mathrm{Ca}}{|\mathbf{M}_0|}\frac{\mu-1}{\mu+1}\left[\left(I_0(k)-\frac{2}{k}I_1(k)\right)|\mathbf{M}_0^{4,1}|+I_1(k)|\mathbf{M}_0^{4,2}|\right]+\frac{k\mathrm{Ca}}{\mu+1},\\
q_{32} &= \frac{\mathrm{Ca}}{|\mathbf{M}_1|}\frac{\mu-1}{\mu+1}\left[\left(I_1(k)-\frac{3}{k}I_2(k)\right)\left(|\mathbf{M}_1^{3,1}|+|\mathbf{M}_1^{5,1}|\right)\right.\\
&\qquad\left.+I_2(k)\left(|\mathbf{M}_1^{3,2}|+|\mathbf{M}_1^{5,2}|\right)+I_1(k)\left(|\mathbf{M}_1^{3,3}|-|\mathbf{M}_1^{5,3}|\right)\right]\\
&\quad-\frac{k\mathrm{Ca}}{|\mathbf{M}_1|}\frac{\mu-1}{\mu+1}\left[\left(I_1(k)-\frac{1}{k}I_0(k)\right)|\mathbf{M}_1^{4,1}|+I_0(k)|\mathbf{M}_1^{4,2}|+I_1(k)|\mathbf{M}_1^{4,3}|\right]\\
&\quad-\frac{k\mathrm{Ca}}{\mu+1},\\
q_{33} &= \frac{k^2}{|\mathbf{M}_1|}\left[\left(I_1(k)-\frac{3}{k}I_2(k)\right)|\mathbf{M}_1^{6,1}|+I_2(k)|\mathbf{M}_1^{6,2}|+I_1(k)|\mathbf{M}_1^{6,3}|\right].
\end{aligned}
$$

$a_0 = 1$

$a_1 = -(q_{11}+q_{22}+q_{33})$

$a_2 = q_{11}q_{22}+q_{11}q_{33}+q_{22}q_{33}-(q_{12}q_{21}+q_{23}q_{32})$

$a_3 = q_{11}q_{23}q_{32}+q_{33}q_{12}q_{21}-q_{11}q_{22}q_{33}$

For the special case$k=0$, for $m\geq 2$:

$$
\mathbf{M}_{m;k=0} = \begin{pmatrix}
1 & \frac{m}{2(m+1)} & -1 & -\frac{m}{2(m-1)}\\
-1 & -\frac{m+2}{2(m+1)} & -1 & -\frac{m-2}{2(m-1)}\\
2\mu(m-1) & m\mu & -2(m+1) & -m\\
2\mu(m-1) & \mu(m-2) & 2(m+1) & m+2
\end{pmatrix}
$$

References

[1] F. Savart, Annal. Chim. Phys. 53 (1833) 337-386.

[2] J. Plateau, Acad. Sci. Bruxelles Meḿ. 23 (1849) 5.

[3] L. Rayleigh, On the stability of liquid jets, Proc. London Math. Soc. 10 (1878) 4-18.

[4] L. Rayleigh , On the instability of a cylinder of viscous liquid under the capillary force, Phil. Mag. 34 (1892) 145-154.

[5] S. Tomotika, On the instability of a cylindrical thread of a viscous liquid surrounded by another viscous fluid, Proc. Roy. Soc. A 150 (1935) 322-337.

[6] B.J. Meister, G.F. Scheele, Generalized solution of the Tomotika stability analysis for a cylindrical jet, AIChE Journal 13 (1967) 682-688.

[7] C.M. Kinoshita, H. Teng, S.M. Masutani, A study of the instability of liquid jets and comparison with Tomotika's analysis, Int. J. Multiphase Flow 20 (1994) 523-533.

[8] S. Tomotika, Breaking up of a drop of viscous liquid immersed in another viscous fluid which is extending at a uniform rate, Proc. Roy. Soc. A 153 (1936) 302-318.

[9] T. Mikami, R.G. Cox, S.G. Mason, Breakup of extending liquid threads, Int. J. Multiphase Flow 2 (1975) 113-138.

[10] D.V. Khakhar, J.M. Ottino, Breakup of liquid threads in linear flows, Int. J. Multiphase Flow 13, 71.

[11] J. Eggers, Nonlinear dynamics and breakup of free surfaces flows, Rev. Mod. Phys. 69 (1997) 865-929.

[12] A. Frischknecht, Stability of cylindrical domains in phase-separating binary fluids in shear flow, Phys. Rev. E 58 (1998) 3495-3514.

[13] T. Hashimoto, K. Matsuzaka, E. Moses, A. Onuki, String phase in phase-separating fluids under shear flow, Phys. Rev. Lett. 74 (1995) 126-129.

[14] K.B. Migler, String formation in sheared polymer blends: Coalescence, breakup, and finite size effect, t Phys. Rev. Lett. 86 (2001) 1023-1026.

[15] J.A. Pathak, K.B. Migler, Droplet-string deformation and stability during microconfined shear flow, *preprint Langmuir.* (2003).

[16] A.Y. Gunawan, J. Molenaar, A.A.F. van de Ven, In-phase and out-of-phase break-up of two immersed liquid threads under influence of surface tension, Eur. J. Mech. B/Fluids 21 (2002) 399-412.

[17] A.Y. Gunawan, J. Molenaar, A.A.F. van de Ven, Break-up of a row of equally spaced immersed threads, RANA 02-08 Eindhoven University of Technology (2002).

[18] Chandrasekhar S., Hydrodynamic and hydromagnetic stability, Dover, New York, 1961.

[19] A.Y. Gunawan, J. Molenaar, A.A.F. van de Ven, Dynamics of a polymer blend driven by surface tension:Part 2 The zero-order solution, RANA 01-20 Eindhoven University of Technology (2001).

[20] D.R. Merkin, Introduction to the theory of stability, Springer, New York, 1997.

[21] A.Y. Gunawan, J. Molenaar, A.A.F. van de Ven, Note on the breakup of immersed threads in the absence of viscosity differences, RANA 02-23 Eindhoven University of Technology (2002).

[22] G.N. Watson, A treatise on the theory of Bessel functions, 2nd edition, University Press, Cambridge, 1966.